arXiv:1603.02539v1 [physics.flu-dyn] 8 Mar 2016

A Lagrangian Dynamic Mode Decomposition

Jörn Sesterhenn and Amir Shahirpour
Institut für Fluidmechanik und Technische Akustik
TU Berlin

Abstract

Temporal or spatial structures are readily extracted from complex data by modal decompositions like POD or DMD. Subspaces of that decompositions serve as reduced order models and define spatial structures in time or temporal structures in space. Convecting phenomena pose a major problem to those decompositions. A structure travelling with a certain group velocity will be perceived as a plethora of modes in time or space respectively. This manifests itself for example in poorly decaying Singular Values when using a POD. The poor decay is very counter-intuitive, since we expect a single structure to be represented by a few modes. The intuition proves to be correct and we show that in a properly chosen reference frame along the characteristic defined by the group velocity, a POD or DMD reduces moving structures to a few modes, as expected. Beyond serving as a reduced model, the resulting entity can be used to define a constant or minimally changing structure in turbulent flows. This can be interpreted as an empirical counterpart to exact coherent structures.

We present the method and its application to a the head vortex of a compressible starting jet.

1 Introduction

Three things come together in this article: so called coherent structures, modal decompositions, and model reduction. The principal aim of this exercise is to extract Lagrangian structures from turbulent flows along characteristics having the slope of the group velocities. Several modes travelling along such a characteristic and interacting amongst them, shall be defined as an empirical coherent structure. The constituent three parts shall be discussed briefly.

Turbulent flows appear to be stunningly complex, but even if a measurement of some quantity appears to be random, it is the outcome of a repeti-

tive and recursive application of a few simple rules considered to be coherent structures in the flow [8], [3]. Relying basically on hot wire measurements and simple flow visualisation measurements, it was extremely difficult to come up with an idea of what structures are behind the observed quantities in turbulent flows, and it was not until the advent of PIV and Numerical Simulations, that the idea of a coherent structure replaced the vague "eddy" in literature. Using those new tools, so called "hairpin vortices" [1] and other coherent structures were described. The availability of the strain rate tensor $S_{ij} = \frac{1}{2}\left(\frac{\partial u_i}{\partial x_j} + \frac{\partial u_j}{\partial x_i}\right)$ from numerical simulations, made the analysis and perception of thoses structures acessible [4] and enabled their visualisation.

Fabian Waleffe [9] computed those structures as fixed point solutions travelling in the flow. This route has been successfully followed such that today exact coherent structures can be computed for relatively high Reynolds numbers [2].

On the other hand, data driven methods were adapted from other field of science to extract structures from turbulent flows. Proper orthogonal decompositions were the first to be introduced to fluid dynamics by Lumley [5]. These patterns however lack dynamics and have problems with convective flows. The first drawback hampers the construction of reduced models of the flow, and in consequence the success was there, but limited. This problem was addressed by the introduction of Dynamical Modes [7]. The difficulties of these methods to describe convective phenomena remained and is what will be discussed and solved in the present paper.

2 The problem

From an empirical point of view we may define a structure as something in space which appears somehow recognisable elsewhere at a later time. A most strict example would be a solution $u(x,t) = u(x-\lambda t)$ to the convection equation

$$\partial_t u + \lambda \partial_x u = 0. \tag{1}$$

Even when nonlinearly distorted, damped and dispersed, e.g. for the Korteweg – de Vries – Burgers equation

$$\partial_t u + u\partial_x u - \nu\partial_x^2 u + \delta\partial_x^3 u = 0, \tag{2}$$

it is possible to find an analytic solution fitting the above definition in form of a soliton. A solution developing from a given initial condition will serve as an introductory example below. But even in in more complex situations, for

example a boundary layer, the flow exhibits structures which lack an analytic solution, but clearly fit the above definition. They might be found as fixed point solutions of the Navier-Stoles equations. In what follows, concentrate on the general case, where we do not have descriptive equations — yet. Our main example will be the vortex ring of a starting supersonic jet. Imagine a shorter or longer pulse of high pressure from an orfice. If the pulse is short, a laminar vortex ring forms. If the pulse is long, a jet will follow the vortex ring and both, vortex ring and jet will become turbulent, if the Reynolds number is sufficiently high. POD, DMD or other model reduction techniques should then easily reduce flows containing those structures. The structure, being the principal mode, modified to some degree by higher modes.

Unfortunately, this is not so. The failure can be demonstated for already for a solution of the KdVB–equation (2). We have chossen the parameters $\nu = 5 \times 10^{-4}$, $\delta = 4 \times 10^{-5}$ and initial condition $u(x,0) = 1 + \alpha e^{-(x-x_o)/\beta^2}$ where $\alpha = 0.1$ and $\beta = 0.03$.

The solution at $t = 0.5$ is given in figure 1, which is distorted, damped and dispersed, but has primarily experienced a shift in x. It would still qualify as a an evolving structure in space and time. A POD of the data

$$X = [u(x,t_0), u(x,t_1), ...u(x,t_{n-1})] \tag{3}$$

using an SVD

$$X = U\Sigma V^T \tag{4}$$

yields the poorly reducing singular values, depicted in figure 2. The POD-modes being an average over all shifted solutions and necessary distortions therefor sum up to the desired solution. This is illustrated in figure 3. The dominant mode appears to be the swallowed elephant in the larger subfigure. Any real instance in time is made up by subtracting a large number of modes like the two depicted following subfigures. The resulting linear combination will not yield zero in may spatial locations and give rise to substantial spurious structure, where there should be none. A DMD along t suffers from the same problem.

3 A remedy

The main problem above comes neither from the non linearity nor the other factors rather than the mere translation. That the flow has a relatively simple structure is easily guessed from the characteristic diagram 4. In fact, solutions travel relatively unmolested in $\tau = x - \lambda t$-direction. Generally

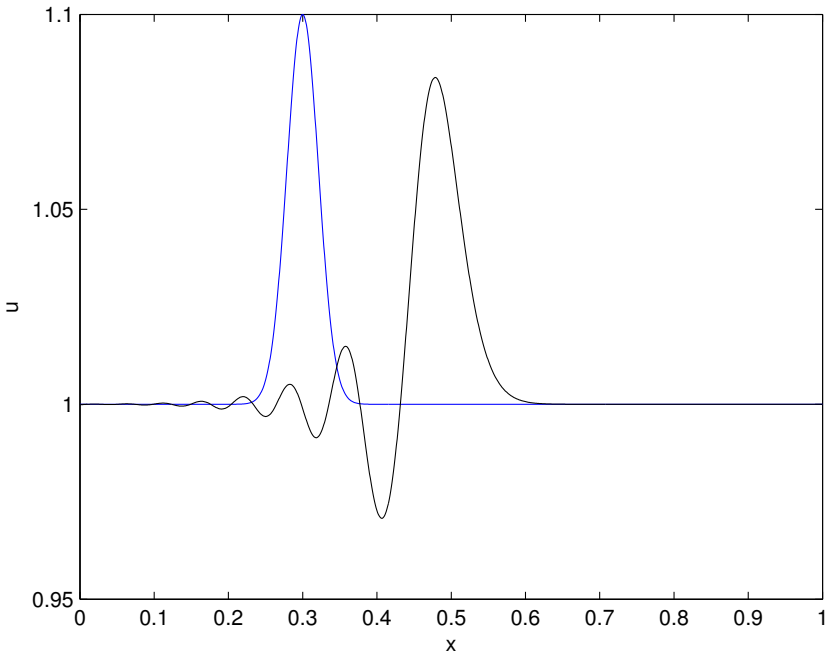

Figure 1: Solution (black) to equation 2 for a Gaussian initial condition (blue)

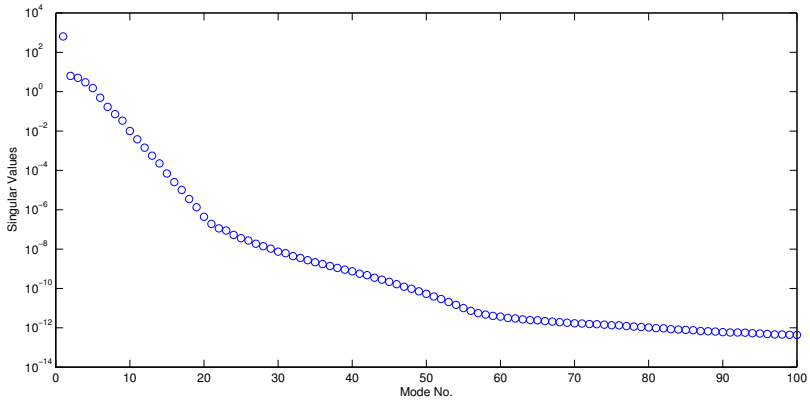

Figure 2: Singular Values of snapshots of solutions to equation (3)

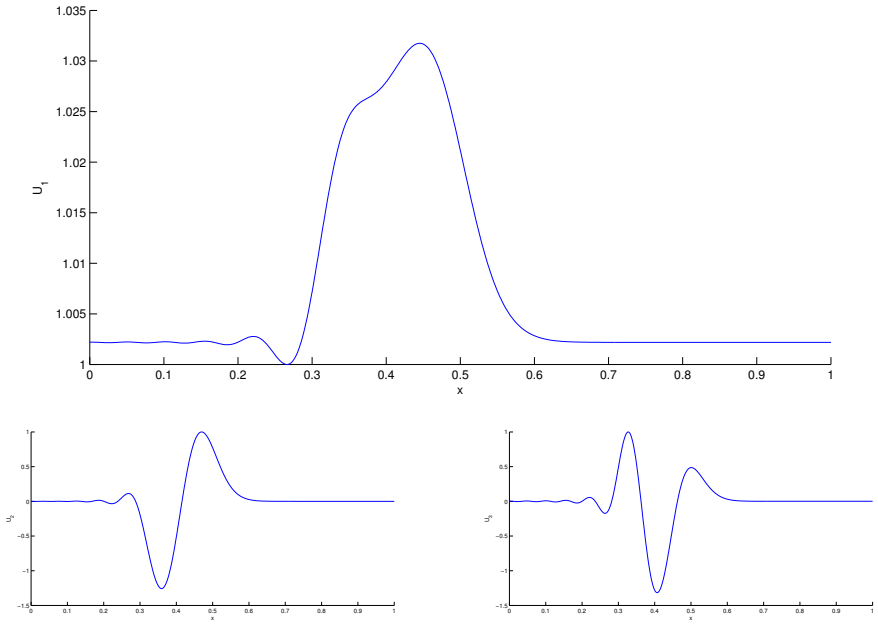

Figure 3: First three POD modes of solution of equation (3)

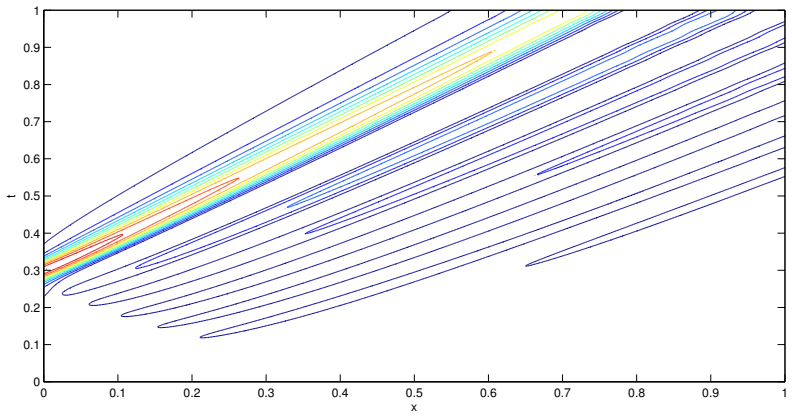

Figure 4: Characteristic diagram of the solution

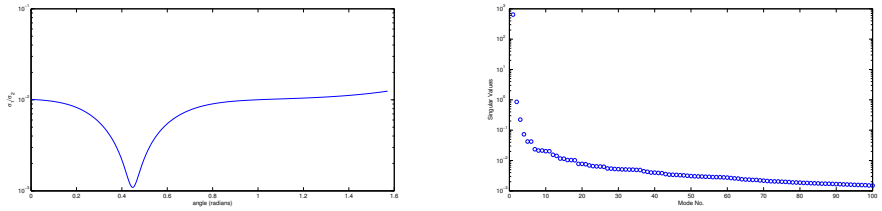

Figure 5: Drop of singular values for varying angles (left) and when aligned with the flow direction in space and time (right)

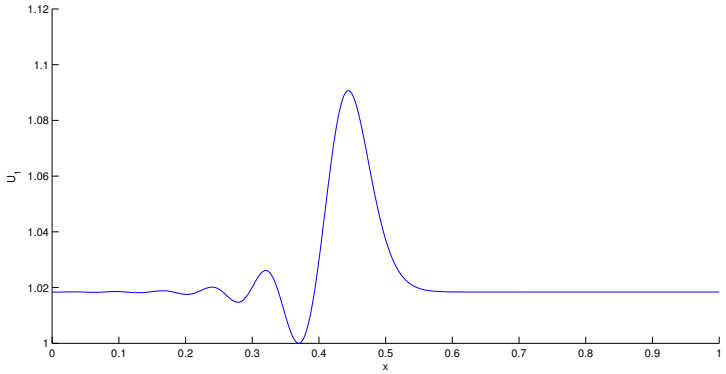

Figure 6: KdVB-Structure

speaking, if a structure travels in time along the direction given by the wave-vector κ, the modal decomposition is to be sought in a plane normal to that direction in space-time

$$x_i = \{t, x_1, x_2, x_3\} \qquad i = 0...3. \tag{5}$$

Given the example above, the ratio of the first to second singular value of eq.(3) are shown in figure 5. There is a dramatic drop when the proper direction is chosen for the snapshot direction. *The essence of the menthod presented here, is to perform a modal decomposition along that direction and later transformed back into pysical space.*

After that operation, the first singular vector, shown in figure 6, looks as expected for the structure of the solution of the KdVB-equation (2). Higher modes drop of fast and minimally change the overall shape of the mode. It should be noted that figure 6 represents the spatio-temporal structure. A back transform to physical space will be necessary to either see the temporal

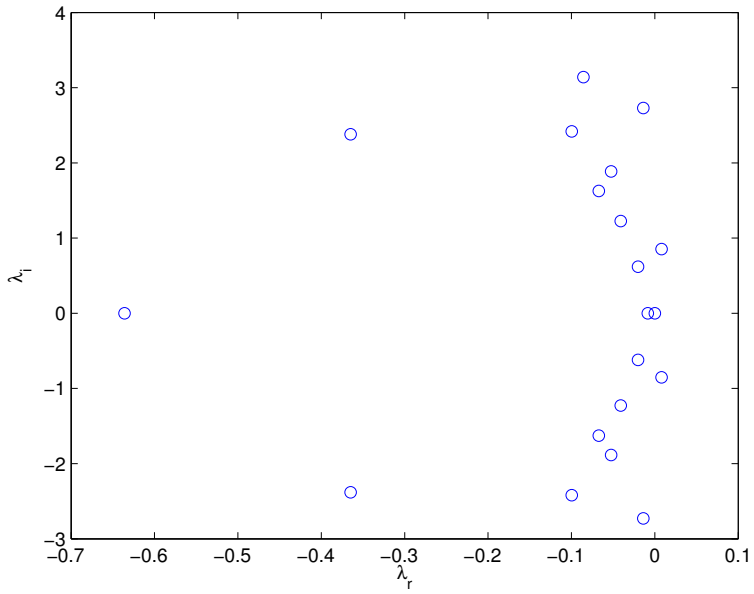

Figure 7: DMD-Spectrum of the development along the τ direction

evolution in a given space interval or conversely the spatial changes in a time interval.

The development of the mode while travelling can better be analysed using a DMD (rather than a POD) along that direction. To that end we assume a linear relationship of the rotated snapshots

$$X_{0..n} = \{u(\xi, \tau_o), u(\xi, \tau_1)...u(\xi, \tau_n)\} \tag{6}$$

as

$$X' = AX \tag{7}$$

with X and X' being the first and last n snapshots in $X_{0..n}$ and approximate the transition matrix using the projected matrix

$$\tilde{A} = U^T A U = U^T X' V \Sigma^{-1}, \tag{8}$$

or another standard method to obtain the DMD. *The important step is to take the columns of $X_{0..n}$ normal to the characteristic direction and the rows along it.* Note that the resulting structures are defined in planes normal to the group velocity of the structure in space-time. That means they have no

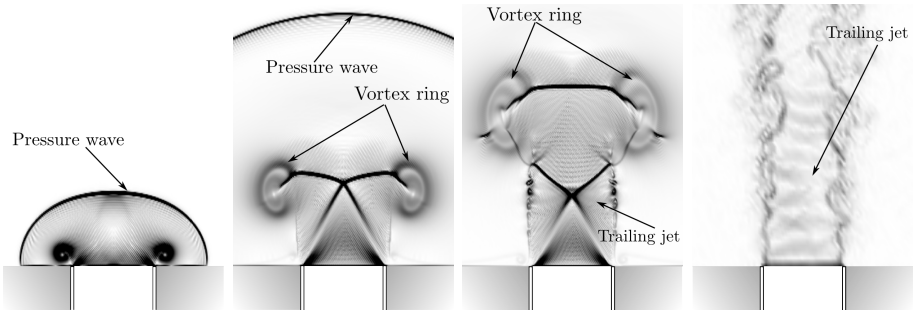

Figure 8: Evolution of the starting Jet

imediate temporal or spatial interpretation. If, for example, a structure is running right to left, the values at the top of the snapshots correspond to a later time than those at the bottom.

4 Results for the Starting Jet

Now we turn to the example of a starting jet and apply the method explained above to this three dimensional case. The starting point is a shock tube-like initial condition with two different gases at different pressures on both sides of a membrane. The difference to the shock tube is due to the fact that one side is connected to the ambient instead of another part of the tube. We have chosen a pressure ratio $p_1/p_2 = 3.4$ such that eventually a supersonic jet will develop. The Reynolds number is about $Re = 10000$, based on the fully expanded conditions. One crucial parameter besides the pressure ratio is the non-dimensional mass supply of the jet. It can be expressed as the ratio of length to diameter of the pipe $C = L/D$. If C is close to unity, a vortex ring will form. In order to develop a trailing jet, C needs to be larger than approximately 5.

The temporal evolution is shown in figure 8 as a pseudo-schlieren image in a two dimensional cut through jet and vortex ring. The first image shows the inital pressure wave and the developing vortex ring at the wall. If enough vorticity is generated, the self–induced velocity if the vortex ring makes it accelerate and travel in flow direction, slightly expanding it's diameter. The third picture shows the vortex ring and the trailing jet, which is formed if enough mass is supplied. The last image shows the full jet when the mass supply vanishes and the vortex ring has moved away. We wish roughly to identify the flow in three cases. First for a vortex ring, without trailing jet,

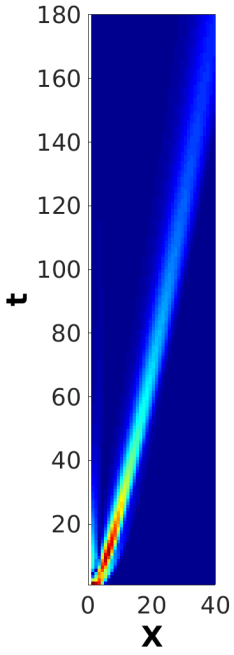

Figure 9: Characteristic diagram of the starting jet. The diagram was extracted at the centre-line of the vortex. On the axis, time– and space indices are shown.

next for the vortex ring with trailing jet at an early and a late state.

4.1 The head vortex in a starting jet

One of the dominant features of the starting jet is the vortex ring. It is initially formed at the tube lip and detaches later to first move with constant speed and finally travels with a velocity decaying as the square root of time. It is now our aim to detect this vortex and describe it with a few DMD modes. The can be seen in the characteristic diagram of the flow given as an $x-t$-diagram of the vorticity along the centre line in figure 9. For a first example, we have chosen a small reservoir with $C = 1$ such that the vortex ring is not followed by a jet and rather travels alone like a ring produced by skillful smokers. We choose for now to determine the optimal direction manually in order not to exhaust the reader by technicalities.

Next, a coordinate transform of the $xyzt$-space into the desired direction has to be performed. One can observe that the group velocity changes with time. Thus also a temporal transformation $t' = \frac{at}{b\sqrt{t}+c}$ with suitable

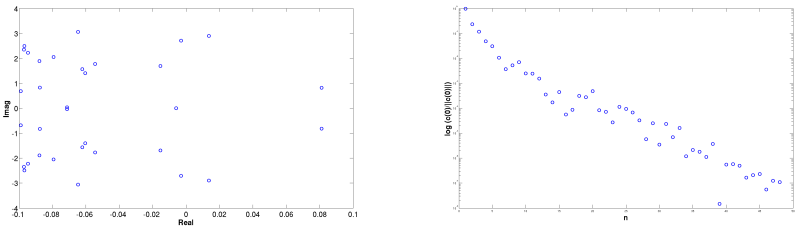

Figure 10: DMD-Spectrum of the head vortex and decay of modal amplitudes for $t = t_0$

coefficients should be employed. This complication is left for later[1] and for now we rotate the $xyzt$-cube of data in such a way that we have a new $\xi\eta\zeta\tau$-cube and choose a satisfyingly straight part on the characteristic for our analysis. Any rotation in four dimensional space can be represented by two rotations in two suitably chosen planes. In our example, where the main flow is in xt-direction, a single rotation in the xt-plane suffices. The procedure is performed as a decomposition of the rotation in three shears $q' = S_1 S_2 S_1 q$ which is fast and accurate [6].

4.1.1 Spectrum and Modal decay of the Lagrangian DMD

A DMD using 100 snapshots in τ-direction yields the spectrum to the left of figure 10. The decay of the DMD modes is plotted in the right diagram of the same figure, where the projection coefficients of the initial snapshot onto the DMD-eigenmodes is shown. They are normalised by the norm off the full mode. It can be observed that the first few modes represent the snapshot up to a relative remainder of less then 10^{-2}.

4.1.2 Reduced order representation of a vortex ring

The first mode of the DMD captures the vortex head ring. Its eigenvalue is close to zero and thus represents the almost invariable vortex head as it is translated downstream. Figure 11 confronts the physical vorticity field with the first two modes. The Lagrangian DMD ($\mathcal{L}$DMD) extracts the vortex ring as the major mode and filters out, both the co-flow at the wall as well as the small trailing vortex, as they have a different decay rate and consequently

[1] Transformation in time can be achieved by choosing the snapshots equidistantly in t' as defined above. Since we have abundant time-steps from our numerical simulation, this is easily done by choosing the right snapshots.

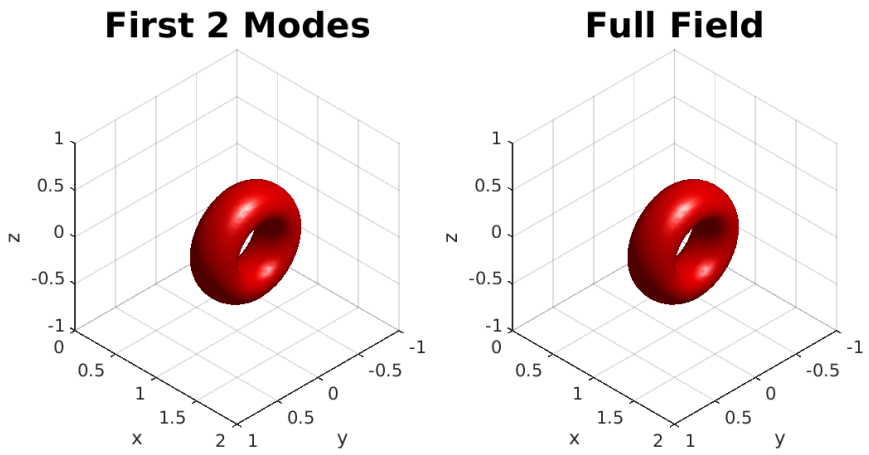

Figure 11: 3D picture of the spatial structure at a given time (right) and the spatial representation of the first mode at the same time (left) both plots show the isosurface of absolute vorticity.

constitute other modes. Already two modes render the differences invisible in the given 3D-plot. In in a 2D plot in figure 12 the correspondence is also very good.

4.1.3 Reduced order representation of the full vortex head at an early time

Next a starting jet with $C > 1$ is presented for an early and a late time. This corresponds to a laminar and a turbulent vortex head. For sake of simplicity we will show 2D cuts of the flow field only in what follows. The reconstruction of the first few modes in spact is shown in figure 13. The figure shows the first two modes as a contour plot of vorticity magnitude. They are almost indistinguishable from the full field, which is depicted in the left plot. These results have to be confronted with the Eulerian DMD results which are given in figure 14. It can be observed that the DMD introduces spurious shadows ahead of the vortex ring. They need to be cancelled out by many modes, but even ten modes are not sufficient. This can be anticipated also from the decay rate given in the right of the same figure.

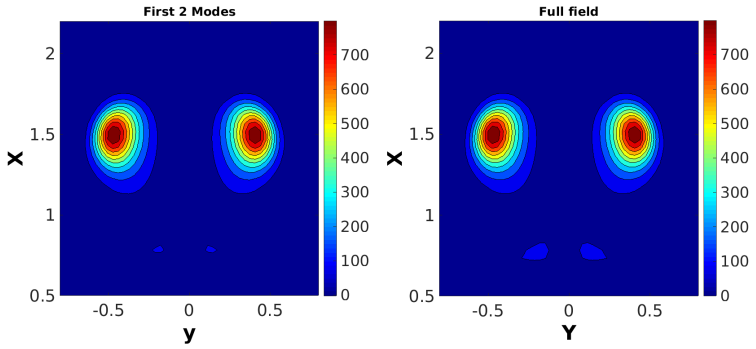

Figure 12: 2D contour plot of vorticity for modes 1-2 for the Lagrangian DMD The right figure depicts the original flow-field.

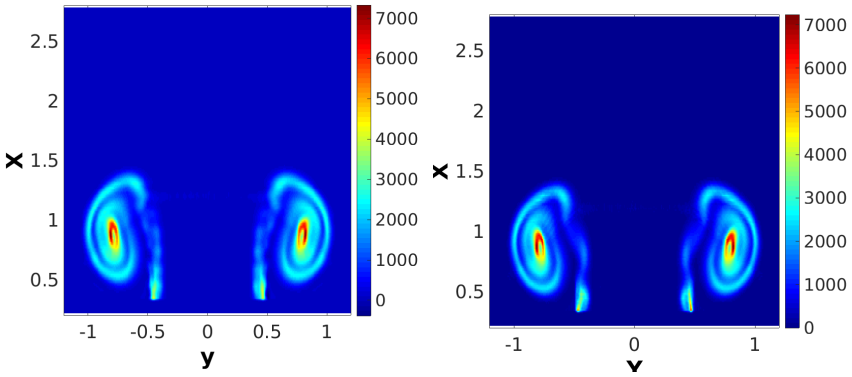

Figure 13: 2D contour plot of vorticity for modes 1-3 for the Lagrangian DMD for time $t = 35$. The right figure depicts the original flowfield.

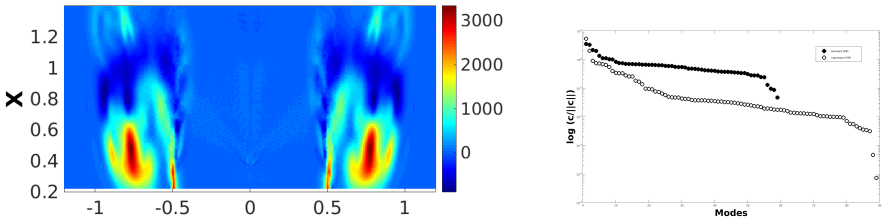

Figure 14: 2D contour plot of vorticity for modes 1-10 for the Eulerian DMD The right figure depicts the decay rates.

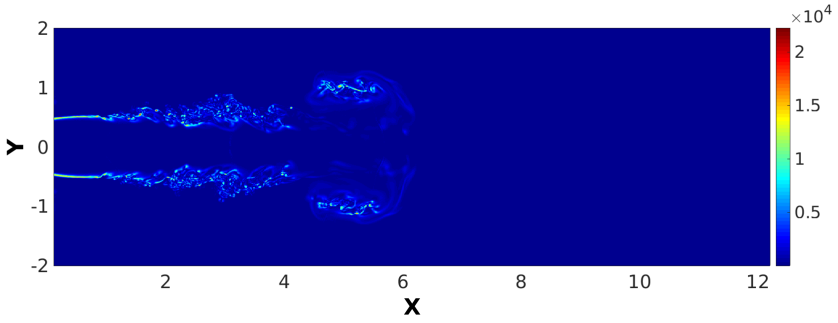

Figure 15: Evolution of the starting Jet

4.2 The fully turbulent developed vortex head

The situation is more complicated but not essentially different for the later turbulent stage of the developed jet. A cut through the full jet is shown in figure 15. The shear layer of this jet is entrained in the vortex head and renders it unstable. One can still see the main structure of the vortex ring, but the entrained shear layer modes have lead to internal turbulent structures.

The characteristic diagram along the jet axis is shown in figure 16. One can observe more than one structure travelling with different velocities. By inspection one can distinguish the acoustic wave, the head wave, shock cells and some other events. The vortex head in the characteristic diagram was

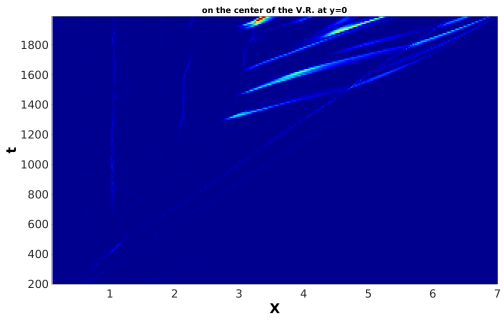

Figure 16: Characteristic diagram along the jet axis

identified again by inspection. Also here, the vortex head is extracted nicely in a single mode. The fine scale turbulent structure is not part of the head, moreover, it moves with a slower group velocity as it travels backwards with respect to the main head motion. That means the internal structure of the jet head suffers again from the same deficiencies as did the whole structure before. In principle one should extract those structure using their characteristic velocity. But already six modes give a clear resemblance of the full structure. Some of these modes have a positive real part and correspond to break up of the vortex head which is soon to occur. The modes which travel with the same group velocity can as an entity, be defined as an empirical coherent structure. As indicated in section 2, they resemble a travelling structure which changes along its path but remains very well recognisable.

5 Conclusion

Performing a modal decomposition along the characteristic directions given by the group velocity of a structure allows for the extraction of moving features. To this end a rotation in four dimensional space is necessary. In general this can be done by two rotations but as in our case of a jet the main direction coincides with one of the axis, one rotation was sufficient. In this rotated frame a modal decomposition is performed. The head vortex of a starting was extracted with a few modes only and also its apparent instability due to the entrainment of the shear layer was reflected by the growth rates revealed by the DMD. The physical structure is recovered after rotation back into the physical frame.

In this way Lagrangian structures as well as their development along their path can be described. The method can be used for the definition of

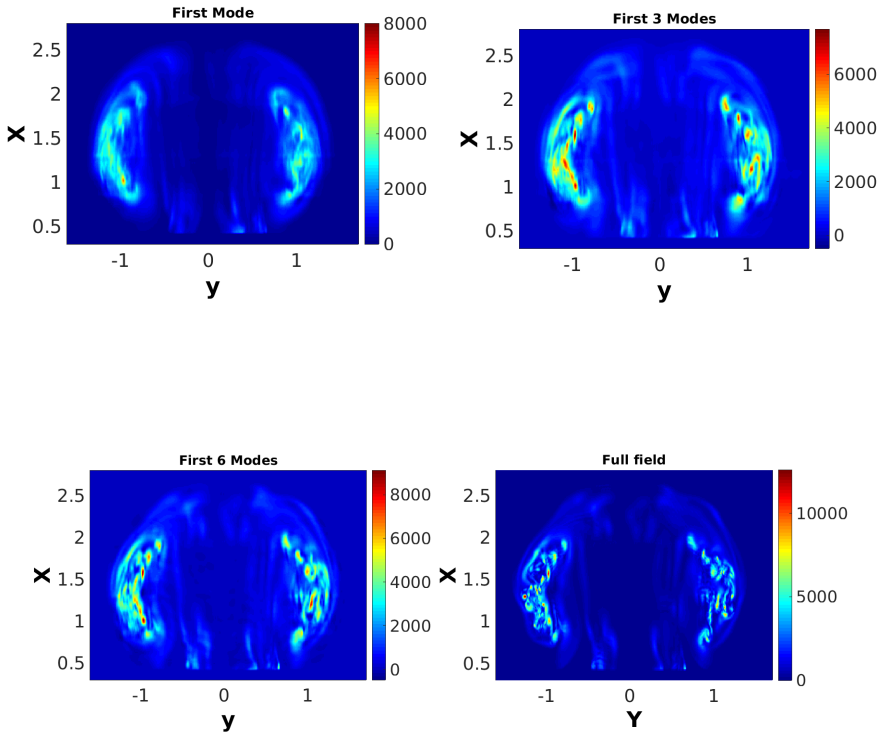

Figure 17: Reconstruction of the trailing vortex for $t = 65$. On the left is the first spatial mode on the top right the first three. At the bottom is a recostruction of six modes along with the full flow field.

empirical coherent structures given as a reduced model described by a few modes, as well as constructing reduced modes for control or other purposes.

References

[1] R Adrian. Hairpin vortex organization in wall turbulence. *Phys. Fluids*, 2007.

[2] M. Avila, F. Mellibovsky, N. Roland, and B. Hof. Streamwise-localized solutions at the onset of turbulence in pipe flow. *Physical Review Letters*, 110(22), 2013.

[3] B. J. Cantwell. Organized motion in turbulent flow. *Annu. Rev. Fluid Mech.*, 13:457, 1981.

[4] M. S. Chong, a. E. Perry, and B. J. Cantwell. A general classification of three-dimensional flow fields. *Physics of Fluids A: Fluid Dynamics*, 2(5):765, 1990.

[5] J. L. Lumley. The structure of inhomogeneous turbulent flows. In A. M. Yaglom and V. I. Tararsky, editors, *Atmospheric Turbulence and Radio Wave Propagation*, Moscow, 1967. Nauka.

[6] AW Paeth. *Graphics Gems*, chapter A fast algorithm for general raster rotation. Academic Press, 1990.

[7] P. J. Schmid and J. L. Sesterhenn. Dynamic mode decomposition of numerical and experimental data. *Bull. Amer. Phys. Soc*, 2008.

[8] A. A. Townsend. *The Structure of Turbulent Shear Flow,*. Cambridge University Press, Cambridge, 2 edition, 1976.

[9] Fabian Waleffe. Three-dimensional coherent states in plane shear flows. *Phys. Rev. Lett.*, 81(4140), 1998.